A Partition-based Mobile Crowd Sensing-enabled Task Allocation for Solar Insecticidal Lamp Internet of Things Maintenance

Yuanhao Sun, Edmond Nurellari, *Member, IEEE*, Weimin Ding* and Lei Shu*, *Senior Member, IEEE*, Zhiqiang Huo

***Abstract*—Solar Insecticidal Lamps Internet of Things (SIL-IoT) is a new green prevention and control technology for pest management. In the implementation of SIL-IoT to large-scale regions, two practical issues remain to be solved, i.e., *i)* scheduling the cleaning tasks of SILs periodically; and *ii)* minimizing the insecticidal efficiency reduction over time. As smartphones are widely available among farmers across the globe, Mobile Crowd Sensing (MCS) for agricultural data collection becomes a cost-effective and efficient solution by integrating participatory sensing based on a large group of individuals. This paper proposes an MCS-enabled framework to address the SIL Maintenance Problem (SILMP) and perform system analysis by considering both the partition structure of farmland and the insecticidal efficiency of SILs. In addition, considering the farmland's practical natural geographical features, we propose dividing the regions of interest into numerous subareas, where each subarea can be considered a separate partition. Finally, we formulate the SILMP framework as two sub-problems, i.e., path planning and task selection, and propose two different methods to tackle each problem based on the concept of greedy algorithm. Simulation results show that our proposed methods have improved performance in the trade-off between task cost and insecticidal efficiency and outperform the three selected baseline algorithms.**

***Index Terms*—Task allocation, mobile crowd sensing, smart agriculture, path planning, combinatorial optimization, solar insecticidal lamps maintenance problem**

I. Introduction

Solar Insecticidal Lamps Internet of Things (SIL-IoT) [1] is a green insecticidal technology in the smart agriculture domain [2]. Due to its high efficiency in insect killing, the SIL-IoT has drawn considerable attention from both academia and industry. Unlike traditional chemical pesticides, SIL-IoT physically kills insects and dynamically reports critical insecticidal information, e.g., insecticidal destiny over time, in real-time. Benefiting from these factors, the SIL-IoT becomes a promising solution to revolutionize traditional farming. In the implementation of such a SIL-IoT system, there still exist two primary problems to be solved. First, the corpses of killed pests, which may stick to the high-voltage metal mesh of Solar Insecticide Lamps (SILs) over time, will eventually cause a short circuit and cause potential (costly) damage to SILs, as shown in Fig. 1. Second, the accumulation of corpses over time will also cause SILs to attract and accumulate pests while the efficiency degrades significantly, i.e., eventually, over time, unable to kill them. At the moment, the most generally utilised approach for SIL maintenance, e.g., once a weak, is performed proactively by professionals and engineers. This method, however, is costly and cannot meet the demand for timely maintenance in some cases, particularly in a large-scale Regions of Interest (ROI) implementation. As a result, intelligent and cost-effective automatic maintenance methods are required to increase the operational lifetime and efficiency of the SIL.

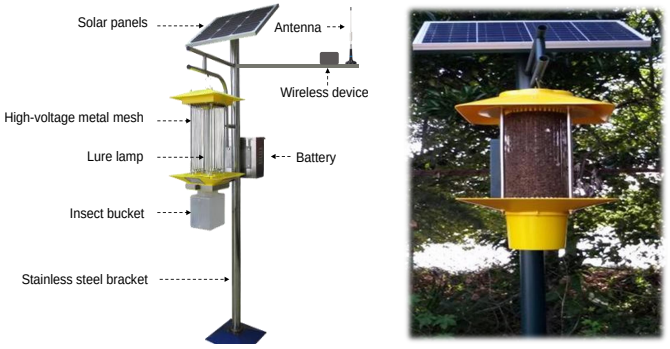

(a) SIL system

(b) SIL covered by the corpses of killed inspects

Fig. 1. An illustration of a typical SIL application and a case where the SIL is covered by the corpses of killed inspects.

Mobile Crowd Sensing (MCS) performs large-scale and complex sensing tasks using mobile devices that enable both high mobility and reliability [3], e.g., smartphones, wearable devices, and robotics. Currently, the applications of MCS are mainly considered for the urban public areas [4] and the industrial scenarios [5] while agricultural considerations are scarce. Few works are reported applying MCS in agricultural scenarios. In our previous survey paper [6], by comparing MCS with existing data collection methods in agriculture, we analyzed the benefits and crucial factors of applying

Y. Sun is with the College of Engineering, Nanjing Agricultural University, Nanjing, 210095, China and with the School of Engineering, University of Lincoln, Lincoln, LN6 7TS, United Kingdom (e-mail: yhsun.nau@outlook.com).

E. Nurellari is with the School of Engineering, University of Lincoln, Lincoln, LN6 7TS, United Kingdom (e-mail: enurellari@lincoln.ac.uk).

Corresponding authors: W. Ding is with the College of Engineering, Nanjing Agricultural University, Nanjing, 210095, China (e-mail: wmding@njau.edu.cn) and L. Shu is with the College of Artificial Intelligence, Nanjing Agricultural University, Nanjing 210095, China, and also with the School of Engineering, University of Lincoln, Lincoln, LN6 7TS, United Kingdom (e-mail: lei.shu@njau.edu.cn).

Z. Huo is with the Institutional Research Information System, University College London, London, United Kingdom (e-mail: z.huo@ucl.ac.uk).

MCS to collect agricultural data, proposing several potential applications and open research issues. This paper focuses on using MCS technology to solve the problem existing in an actual agricultural scenario. Specifically, we exploit the SIL-IoTs features, e.g., reporting insecticidal number, proposing an MCS-enabled approach to the Solar Insecticidal Lamps Maintenance Problem (SILMP). The maintenance task in such an MCS-enabled solution compromises: *i)* via acquiring the insecticidal number of each SIL node, MCS platform can evaluate and predict the condition of all SILs, reporting the maintenance information, e.g., geographical coordinate and serial number; *ii)* for an MCS platform, allocating tasks to optimal users is the basic requirement for achieving large-scale sensing and reducing the total sensing cost. Similarly, to maintain these SILs with minimum cost, an MCS platform needs to optimally match participants with maintenance information. Participants are expected to reach the RoI for conducting assigned maintenance activities in this work, where RoI is defined as the location of SIL of need to be maintained. The maintenance work comprises photographing the insecticidal state, e.g., insecticidal species, and cleaning both the metal mesh and the insect bucket.

A. Related Works

Designing appropriate task allocation algorithms is a vital approach for efficiently maintaining the SILs, which is useful for lowering maintenance costs. As previously stated, in SILMP, participants must reach RoI to accomplish the duties of photography and cleaning, which may be described as an orienteering and combinatorial optimization problem. Furthermore, before implementing the proposed allocation algorithms in real-world MCS systems, they should be evaluated. Thus, the existing work is addressed in two parts: 1) task allocation for the orienteering and combinatorial optimization issue; 2) algorithm evaluation.

1) Task Allocation for the Orienteering Problem: Authors in [7] proposed a task management framework that aimed to maximize the task completion rate and the coverage area of sensor trajectories simultaneously. Authors in [8] aimed to maximize the platform profit, which defined as incomes from task requester minus rewards paid to participants, under the limitation of participant travel distance budget. They proposed an approximate algorithm by applying the local ratio technique such that the task allocation and itineraries for all participants are determined in an offline manner. Authors in [9] aimed to maximize the number of completed tasks and also minimize the sum of travel distance of all mobile participants, which first used the minimum cost maximum flow theory to model the problem. They proposed a heuristic solution that restricts each mobile participant to select tasks from his/her closest k tasks. Authors in [10] studied the moving path scheduling problem to minimize the total task tardiness penalty and designed a genetic algorithm to address this problem. A common assumption on participant movement in [8] [10] is that mobile participants only have starting points but without destination points. Authors in [11] focused on the online task assignment where mobile participants and tasks arrive dynamically. The objective is to maximize total task quality under constraints of participants travel distance budgets and task performing capacity (the maximum number of tasks that each participant can perform during an itinerary). In [11], a Quality-Aware Online Task Assignment algorithm was proposed based on the assumption that each participant has a start point, a destination point, and a travel distance budget. This algorithm used depth-first search with branch and bound for optimal task allocation for each arriving participant. Authors in [29] studied the task allocation and path planning problem in mobile crowdsensing, which aimed to maximize total task quality under constraints of user travel distance budgets designing four online task allocation algorithms.

2) Algorithm Evaluation: The absence of publicly available real-world datasets from applications is one of the most difficult difficulties for the MCS research community in evaluating the task allocation algorithm. Therefore, most experimental evaluations are based on real-world datasets including proprietary data [12] [13], participants historical call records [14] [15] and synthetic data [16] [17]. For real-world datasets, the call records or mobility data is usually based on a real-world dataset, e.g., D4D [18], and Gowalla [19]. D4D dataset is used in the evaluation of task allocation algorithms, e.g., [9] [20] [23], containing two data types. One data type contains information about cell towers, including tower id, latitude, and longitude. The other one contains 50 000 participants phone call records in Ivory Coast. The call records, in fact, do not represent the actual datasets required for the MCS investigations, in which workers respond to assignments provided by the requester. As a result, the generated synthetic data from these research may not accurately replicate the properties of real-world MCS datasets, such as spatial-temporal distribution, budget, and needed quality, and can only be used for a limited number of MCS applications. For the synthetic data, one example is that the authors in [24] presented a toolbox to generate synthetic data for MCS testing, resulting in reproducible research. In addition to a dataset, a popular technique for algorithm evaluation is to compare performance with different baselines under various conditions, such as the number of tasks and workers, worker bandwidth, total incentive budget, and task distribution.

B. Comparison and Challenges

1) Comparison: Currently, existing task allocation algorithms were mainly designed for applications in cities. However, there are apparent differences for MCS applied in between urban area and rural area, as shown in Table I.

In urban areas, many participants working in various industries have smart devices connected with 4G, 5G, or Wi-Fi, and can use the navigation to arrive anywhere. Thus, a task can be completed by multiple participants for ensuring the quality of the task. Generally, participants have no direct affiliation with published tasks because the execution area of these tasks focuses on a public area, e.g., the air quality of cities. Besides, the weather has no apparent effect on performing tasks. For data processing, the missing data in an MCS campaign can be inferred based on the known physical property, e.g., assuming the lost air quality data.

TABLE I
COMPARISON OF MCS APPLIED IN URBAN AREA AND RURAL AREA

Sort	Item	Urban Area	Rural Area
Task	Task objective	Air quality, noise level	Insecticidal information of SILs
	Type of available network	4G, 5G, Wi-Fi	Base station
	Signal quality	Good	Bad
	Path navigation	Available	Unavailable
	Task execution area	Focus on public area	Focus on private area
	Task completion	Multiple participants finish a task	A participant finishes multiple tasks
Participant	Occupation	Work on various industries	Farmers
	Direct affiliation between tasks and participant	No	Yes
	Number of participants	Large	Few
	Weather effect	Unaffected	Have a great effect
Data processing	Missing data	Can be inferred	Cannot be inferred

Rural places, on the other hand, have fewer participants than cities. As a result, in order for an MCS campaign to be successful, a participant must complete many activities. In contrast to urban areas, task execution zones are typically located in farmlands that are owned by farmers. Therefore, participants have a direct affiliation with published tasks. It is worth mentioning that navigation is impossible in fields, and the weather has a notable impact on mission completion. Furthermore, the missing data cannot be inferred due to unknown mechanisms, such as pest distribution and density.

2) Challenges: Based on the above analysis, the existing task allocation algorithms cannot solve the SILMP due to the following problems:

(i) The existing research of path planning for MCS mainly focuses on the sequence of performing tasks instead of how to arrive at the assigned tasks location from the initial location of participants. For the convenience of the calculation, previous studies directly use Euclidean distance between participants and the RoI as the travel distance. However, the existing commercial maps, e.g., Baidu Map and Google Map, lack the critical information of farmland, e.g., ridges. Meanwhile, the shape of ridges in actual farmland are irregular, and participants have to reach the RoI via ridges. Thus, the distance calculated by Euclidean distance directly between tasks and participate is quite different from their actual distance.

(ii) Due to the irregularity of farmlands, it is inaccurate to directly calculate the travel distance between participants and tasks by using Euclidean distance or Manhattan distance. Thus, on one hand, the actual cost of participants cannot be predicted, which will lead to unfair payment and reduce the participants' enthusiasm. On the other hand, the sponsor of the MCS campaign cannot get the optimal allocation scheme for SILMP.

(iii) There are no open simulation data that can be used to evaluate task allocation performance in rural areas.

C. Contribution & Organization

The comparisons between the proposed work and related ones are shown in Table II. The main contributions of this article are summarized as follows:

1) Unlike MCS applied in an urban area, task allocation in a rural area cannot use commercial maps to plan paths directly. Inspired by the natural partition of farmland, this work establishes a novel mathematical farmland model by transforming a plane geographic map of farmland to a set of points.
2) we transfer the SILMP into an orienteering and combinatorial optimization problem to allocate appropriate tasks to participants toward efficient maintenance of the SILs. The purpose of optimization is to maximize the insecticide efficiency of SILs while minimizing total task cost. Then, using the natural partitioning of farms and the concept of face routing, we propose Partition-based Optimal Path Planning (POPP) to rapidly identify the optimum path and Cost-Efficiency-Balance-based Task Allocation (CEBT) to meet the designed goal.
3) The performance of the proposed methods is evaluated using synthetic data based on both the agriculture model and Random Way Point (RWP) mobility model.

TABLE II
FEATURE COMPARISONS BETWEEN OUR WORK AND RELATED WORK

Classification	Related work [11] [29]	Our proposed work
Area	Urban area	Rural area
Scenario	Monitoring air quality	SIL-IoT
participant	Citizens	Farmers
Map	Commercial map	Mapping based on geographic information
Path	Urban roads	Ridges
Distance	Euclidean distance	Real distance

The rest of this paper is organized as follows. Section II reviews related works and summarizes contributions. System model is presented in Section III. The formulation of SILMP and the proposed allocation algorithms are described respectively in Section IV. Simulation results and discussions are shown in Section V. Finally, Section VII concludes this paper and presents future work.

II. System Model

In this study, we use the concept of MCS to maintain SILs that are deployed on a large scale filed. The system model, like traditional task allocation for MCS, includes the task model, participant model, and incentive model. The difference is that the planning path on the ridges based on present technologies is not available. As a result, we present the farmland model in this section to solve the orienteering problem. Notations used in this paper are listed in Table III.

(a)

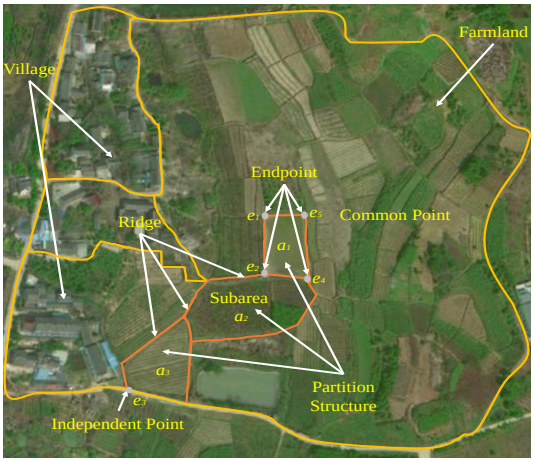

(b)

Fig. 2. (a) An example of actual farmland (This farmland is located in Dong village, Nanjing, China. 118°45′E, 31°99′N) with characteristics of irregular boundary and partition structure. The area of the farmland is about $5.4 \times 10^5\ m^2$. (b) The diagram of actual farmland characteristics. The ridges divide the farmland into many irregular subareas, forming many natural partition structure. Each subarea is a separate partition with a unique predetermined partition number.

A. Farmland Model

Definition 1. *Independent Points (IPs) are the endpoints that belong to a single subarea in the established farmland model.*

Definition 2. *Common Points (CPs) are the endpoints that belong to multiple subareas in the established farmland model.*

Actual farmland A, as shown in Fig. 2 (a)[1], consists of several polygonal subareas, e.g., $A = \{a_1, a_2, a_3\}$. Meanwhile, each subarea can be made up of a set of ordered endpoints, e.g., $a_1 = \{e_1, e_2, e_3, e_4\}$, as shown in Fig. 2 (b). Then, these endpoints can be divided into IPs, e.g., $e_3 \in a_3$, and CPs, e.g., $e_2 \in \{a_1, a_2\}$. Besides, each endpoint also involves location information $L_I^e(x_I^e, y_I^e)$ for calculating the real moving distance of each participant. In this paper, the locations, i.e., longitude and latitude, of these endpoints are calibrated manually based on the satellite image acquired from Baidu Map.

B. Task Model

Since SILs normally work at night, e.g., 7 p.m. to 5 a.m., we assume that daily new tasks (RoIS) are released between 6:00 a.m. and 6:00 p.m. Then, each task $t_k \in T$ has a coordinate and can only be performed once by a participant. It is worth noting that SILs $s_l \in S$ are generally deployed on the ridges of farmland for easy of both the maintenance of SILs and the operation of agricultural machines [25], thus, participants can reach the tasks' location $L_k^t(x_k^t, y_k^t)$ through the ridges.

The critical purpose of maintaining is to ensure that all SILs can work efficiently. In a real SIL-IoT scenario, the insecticidal number can be calculated by the number of Falling Edge Trigger [1], i.e., the number of electric pulse. Nevertheless, the collected data cannot directly reflect the actual situation of killed pests sticking to the high-voltage metal mesh because part of corpses will drop into insect buckets of SILs. Hence, we present the concept of Remaining Insecticidal Efficiency (RIE) to characterize the real-time insecticidal efficiency of SILs. RIE and tasks publishing mechanism can be modelled as Eq. (1) and Eq. (2), respectively.

$$RIE_l = 1 - \frac{M_l \cdot \lambda}{\theta}, \quad M \leq \theta \tag{1}$$

$$T_k = s_l = \begin{cases} 0, & RIE_l > \vartheta \\ 1, & RIE_l \leq \vartheta \end{cases} \tag{2}$$

where RIE_l is the insecticidal efficiency of SIL l, M_l is the number of killed pest of SIL l, λ is the probability of killed pests sticking to the high-voltage metal mesh (adherence rate of killed pests), θ is the upper bound of the number of Falling Edge Trigger. Threshold value ϑ is set to judge the state of each SIL. While $RIE_l \leq \vartheta$, T_k = 1 represents that SIL l needs to be maintained in next sensing period. Then, SIL l is transferred to task k saved in task pool T. Otherwise, T_k = 0, there is no maintenance task generated.

C. Participant Model

For each arrived participant $u_j \in U$, he/she needs to provide an initial location $L_j^{init}(x_j^{init}, y_j^{init})$ and a predetermined destination $L_j^{dest}(x_j^{dest}, y_j^{dest})$, each participate also registers his/her information, e.g., their budget on travelling distance, to the MCS platform. Besides, in rural area, the distribution of participants is uneven. For example, the task close to villages

[1]For this paper, we recommend color printing to enhance the readability.

will be completed by multiple participates. On the contrary, there is few participant to carry out the task far away from villages. Thus, in the SILMP, a participant may be allocated multiple tasks.

D. Incentive Model

The cost of each task includes the travelling cost of the participant and maintenance cost. We assume that the travelling cost is determined directly by the travelling distance of participants and the maintenance cost is a fixed value towards each SIL. Thus, the incentive model is defined as follow:

$$C(j) = d_j^l \cdot c_d + n_t^j \cdot c_s \tag{3}$$

where $C(j)$ is the total reward of participant j finishing all allocated tasks, d_j^l is the travelling distance from participant j's current location to the location of SIL l, c_d is the reward for per unit of travelling distance, n_t^j presents the completed task number of participant j, c_s is the reward for maintaining a SIL.

TABLE III
NOTATIONS

Notation	Description
i	Index of farmland's subareas
j	Index of participants
k	Index of tasks
l	Index of SILs
I	Index of endpoints
L_I^e	Location of endpoint I
IE_k	Insecticidal efficiency of SIL k
u_j^{init}	Initial location of participant j
u_j^{dest}	Predetermined destination of participant j
$d_{u_j}^{t_k}$	Travelling distance from participant j's current location to the location of task k
D_j	Upper bound of travelling distance for participant j
c_d	Reward for per unit of travelling distance
w	The location information of participants
N_p	The number of participants
N_t	The number of tasks
N_{index}^e	The number of endpoints remaining in the current subarea

III. Problem Formulation

In this section, the SILMP is formulated to two subproblems: 1) path planning; 2) task selection. Path planning aims to minimize total task cost by allocating tasks and scheduling paths for each participant with the objective functions formulated as:

$$min\ C \tag{4}$$

Task selection aims to maximize total insecticidal efficiency of maintained SILs with the objective functions formulated as:

$$max\ RIE \tag{5}$$

s.t.

$$\sum_{t_k \in T} d(u_j^{curr}, t_k) \leq D_j \tag{6}$$

$$\sum_{t_k} x_j^k = 1, \quad t_k \in T \tag{7}$$

$$\begin{aligned} L_j^{init}(x_j^{init}, y_j^{init}) \leq w, u_j \in U \\ L_j^{dest}(x_j^{dest}, y_j^{dest}) \leq w, u_j \in U \end{aligned} \tag{8}$$

where Eq. (6) ensures that travel distance constraint of each participate is not violated before he/she reaches his/her predetermined destination. Eq. (7) presents each task can only be completed once. Eq. (8) guarantees both the initial location and the destination of participants are in villages or roads. The SILMP is NP-hard and proved in the next Lemma.

Lemma 1. The SILMP is NP hard:

Proof. The Orienteering Problem (OP) has been proved NP-hard by Golden et al. [26] in 1987. This problem describes that there is a complete graph $G = (V, E)$, including a set of points $V = \{1, ..., n\}$ and a set of edges $E = \{(p, q)|p, q \in V\}$, where 1 is the start point, and n is the destination point. Each point (except beginning point and destination point) has a score s_p. The problem is to maximise the total collected score. The objective function is:

$$max \sum_{p=1}^{n} \sum_{q=1}^{n} s_p x_{pq} \tag{9}$$

where x_{pq} presents whether the edge (p, q) is selected. For the SILMP, we consider a special case of this problem, in which there is only one mobile participant. Then we build a complete graph including three points: the participant's initial point, destination points, and location of unfinished tasks. The value of a vertex (except the participants initial points and destination points) equals its corresponding utility value (specific value of RIE and C). The weights of edges in this graph present the travelling distances between different locations. This particular case is to maximize the total utility value finished by the participant under his/her travelling distance budget. Thus this special case is NP-hard because it can be formulated as the OP. Furthermore, the SILMP for multiple participants is NP-hard since it can be reduced to the OP.

This concludes the proof. ■

IV. Proposed Algorithms

The process of solving the SILMP can be divided into two phases. Phrase 1: search shortest path of participants based on the partition of farmland and the right-hand rule; Phase 2: allocate task considering the trade off between travelling distance of participants and the RIE of SILs.

A. Partition-based Optimal Path Planning (POPP)

Based on the Eq. (4), minimizing the cost of allocated tasks can be further transferred to plan the shortest travelling distance of all participants. Thus, the objective function can also be simplified as:

$$min \sum_{u_j \in U, t_k \in T} d_{u_j}^{t_k} \tag{10}$$

Algorithm 1: Partition-based Optimal Path Planning (POPP)

input : L_j^{init}, L_j^{dest}, t_k, s_l, D_j
output: Travelling distance $d_j^{t_k}$, Sequence of subarea S_i between current location of participants u_j and task t_k

```
d_j^{t_k}* ← ∅; S_i* ← ∅ ;
for k ← 1 to N_ub^t do
    if the number of subarea index for task k > 1 then
        Choose initial subarea a_i satisfying Eq. (14);
        else Apply right hand rule to find a set of subareas satisfying Eq. (6) based on both the current location of participant u_j and the location of task t_k;
    end
    if acc < 0 then
        if N_index^e > 0 then
            Choose next subarea ;
            else S_i* ← a_i;
        end
        else Choose next endpoint;
    end
end
if d_j^{t_k} < D_j then
    d_j^{t_k}* ← d_j^{t_k};
end
return d_j^{t_k}*, S_i*
```

Based on the thought of face-routing [27] while considering the characteristic of partition structure, we propose a partition-based optimal path planning (POPP) algorithm to plan participants' paths. The process of selecting the optimal path planning can be divided into two stages: i) Use the right-hand rule to search valid subareas; ii) Plan path based on the searched subareas. Algorithm 1 gives the procedure for POPP.

1) Right-hand Rule: In this part, we introduce the principle and the judgment of right-hand rule in the established farmland model, as shown in Fig. 3(a).

2) Principle: Like face-routing, an auxiliary line between the beginning and finishing points is set up first. For the convenience of calculation, we select the task (SIL) as the beginning point and the initial location of the participant as the finishing point. According to the known coordinates of these two points, the parameters ξ and ς in the Eq. (11) of the line can be solved easily. Based on the predefined index of each endpoint, we can judge in sequence if these points

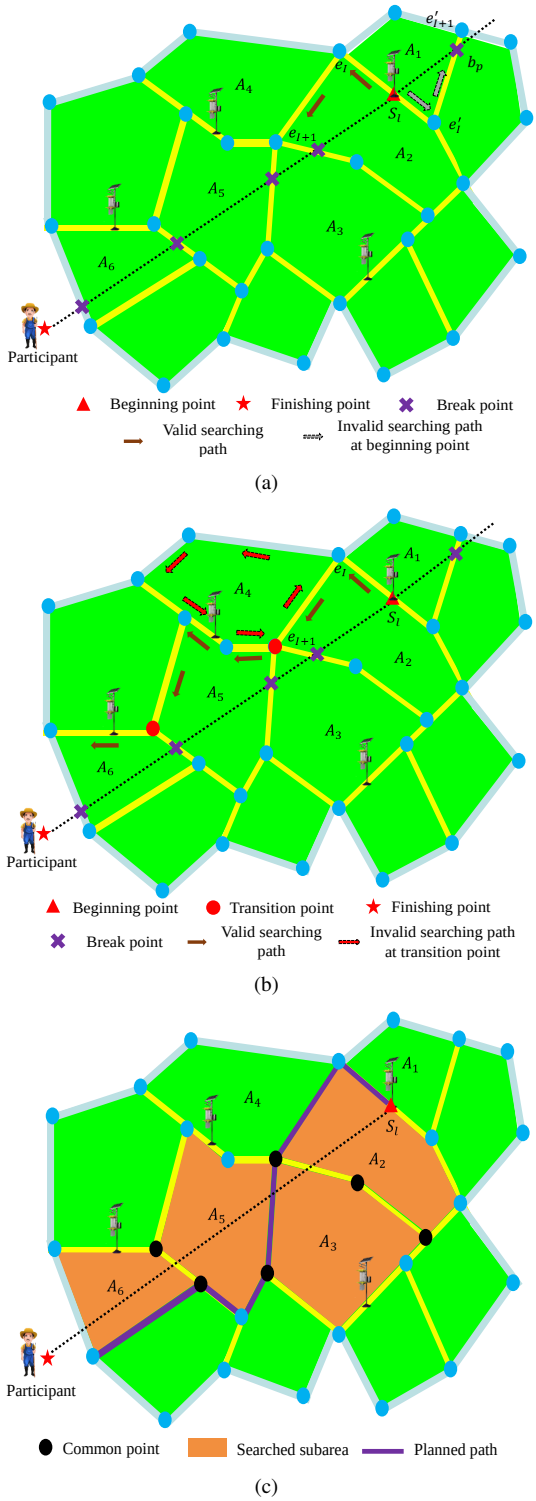

Fig. 3. (a) Judgment at beginning point. (b) Judgment at transition point. (c) The searched subareas and planned path.

meet the requirement of the right-hand rule. For example, we put the coordinates of both e_I and e_{I+1} into the Eq. (11) to gain the eqn_I and eqn_{I+1}, respectively. Then, we put the two calculated values into Eq. (12). If acc is not less than 0, it presents these two points are on the same side of the auxiliary line. We can further judge the next endpoint. Otherwise, we need to rejudge the endpoint e_I in a new subarea.

$$eqn = \xi \cdot x + \varsigma - y \tag{11}$$

$$acc = eqn_I \cdot eqn_{I+1} \tag{12}$$

where acc is a flag for judging whether there is a break point via calculating the product of eqn_I and eqn_{I+1}.

Definition 3. *The beginning point is the first endpoint for the right-hand rule to judge whether the following endpoint is a valid point to path planning.*

Definition 4. *The break point, e.g., b_p, in Fig. 3(a), is met when two adjacent endpoints are distributed on two sides of the auxiliary line.*

Definition 5. *The transition point, e.g., e_{I+1}, is the former point in Eq. (12) when a break point is met.*

STEP 1- Judgment at Beginning Point: In the established model, beginning point may belong to two subareas, e.g., s_l, belongs to A_1 and A_2, simultaneously. Although each subarea can get a solution, there is only one valid solution in these two subareas. To eliminate the invalid solution, we judge the valid subarea of beginning point with Eq. (13) and Eq. (14), where $d(A_i^{e_{I+1}}, u_j^{init})$ presents the distance between endpoint e_{I+1} of subarea A_i and finishing point, $d(A_{i'}^{e'_{I+1}}, u_j^{init})$ presents the distance between endpoint e'_{I+1} of the other subarea $A_{i'}$ and finishing point, $Diff$ is the difference of the two distance. It is worth noting that the value of $I+1$ in $A_i^{e_{I+1}}$ is equal to the value of $I+1$ in eqn_{I+1} when acc is less than 0 in Eq. (12). While $Diff$ is less than 0, it presents that $A_{i'}$ is the valid subarea. Otherwise, the valid subarea is A_i.

$$Diff = d(A_i^{e_{I+1}}, u_j^{init}) - d(A_{i'}^{e'_{I+1}}, u_j^{init}) \tag{13}$$

$$Index\ of\ A = \begin{cases} i', & Diff > 0 \\ i, & Diff < 0 \end{cases} \tag{14}$$

where $Diff$ is a flag to judge which subarea should be selected at the beginning point.

STEP 2- Judgment at Transition Point: While acc is less than 0, it means that the current point is a break-point, the purple cross as shown in Fig. 3 (b), between two adjacent endpoints. In this case, we define the endpoint with red colour belonging to multiple subareas as a transition point, i.e., $e_{I+1} \in \{A_2, A_3, A_4, A_5\}$. When a transition point is met, the proposed algorithm will stop searching in the current subarea, e.g., A_2, record the index of the subarea, and begin exploring a new subarea, e.g., A_4. The subarea, e.g., A_4, is an invalid searching area when the number of searches is equal to the number of endpoints contained in the subarea. Otherwise, a new transition point will be met to continue the investigations in another new subarea. Finally, the search will stop until no new subarea can be found at a transition point. The brown colour arrows and the red colour arrows show the valid searching process and the invalid searching process.

3) Search Subarea and Plan Path: Based on the above principle and judgments, a set of subareas, the orange area shown in Fig. 3 (c), is selected with the specific order, i.e., A_2, A_3, A_5, and A_6. Due to the reduction of subareas, some CPs will be changed to IPs, e.g., endpoint e_I. Besides, participants can only go through ridges to reach the allocated task. Thus, to optimize the path, we can merely utilize the remaining CPs, the black colour points in Fig. 3 (c). In this algorithm, the computational complexity will not increase with the extension of the scenario's scale because the number of the selected subareas is limited under the constraints of travelling distance. Hence, we adopt the Tree Traversal [28] approach to search for the optimal order of endpoints. Finally, the shortest distance in the selected subareas can be calculated according to the sequence of selected endpoints. Hereafter, distance discussed means Euclidean distance.

B. Cost-Efficiency-Balance-based Task Allocation (CEBT)

The key design philosophy of the proposed approach in this paper is to pursue local optimization by allocating each participant with high RIE but low cost tasks on his/her travelling track. To achieve this purpose, we construct a utility function that is the ratio of RIE increment over the travelling distance. The utility for a task t_k and a participant u_j is computed as follows:

$$Utility(u_j, t_k) = \frac{\triangle RIE_k}{d(u_j^{curr}, t_k)} \tag{15}$$

where $\triangle RIE_k$ presents the increased insecticidal efficiency after completing task k, $d(u_j^{curr}, t_k)$ is the distance between the current location of participant j and the location of task k. In this paper, the task with a higher utility value has the higher priority. Hence, by comparing the utility values of different candidate tasks, the task of higher utility value will be selected first as the next task under the travelling distance constraint.

According to the utility function, we propose Cost-Efficiency-Balance-based Task Allocation (CEBT) to allocate tasks to participants. The objective function is transformed to

$$max \sum_{u_j \in U, t_k \in T} Utility \tag{16}$$

Based on the Eq. (16), the final allocation combination set will be output. A flowchart is given to illustrate the solution scheme, as shown in Fig. 4.

V. Evaluation

In this section, firstly, three baseline task allocation methods for comparative studies are introduced. Then, the experimental data and the basic experiment settings are presented. Finally, the effectiveness of our approach is proved via comparing it with the baseline methods.

Algorithm 2: Cost-Efficiency-Balance-based Task Allocation (CEBT)

input : ${d_j^{t_k}}^*$, S_i^*, RIE_k
output: Task sequence T^* on participant u_j's travel path

for $j \leftarrow 1$ **to** N_j **do**
  for $k \leftarrow 2$ **to** N_t **do**
    $d(u_j^{curr}, t_k) \leftarrow {d_j^{t_k}}^*$; $G_k \leftarrow Utility(u_j, t_1)$;
    if $Utility(u_j, t_k) > G_k$ **then**
      $G_k \leftarrow Utility(u_j, t_k)$;
      $T^* \leftarrow t_k$;
      $U^* \leftarrow u_j$;
    end
    Delete task t_k in task pool T;
    if $T == null$ **then**
      return T^*;
      else Continue;
    end
  end
  Reorder the tasks allocated to participant j in T^* ;
end
return T^* ;
Draw the path based on the combination and the sequence of both tasks and participants.

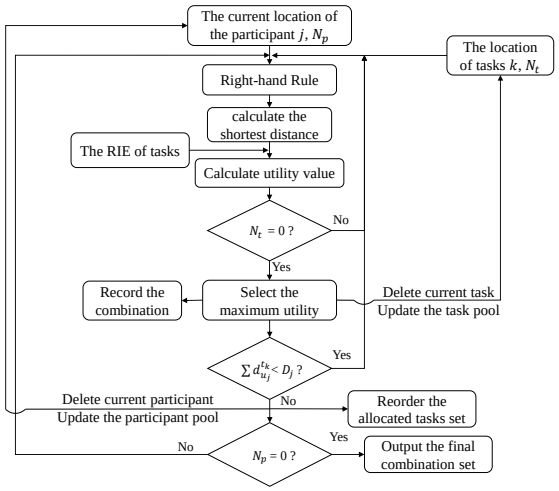

Fig. 4. A flowchart for the solution of SILMP.

A. Baselines

Three baseline task allocation methods are provided for evaluation as follow:

1) Maximize the Increment of RIE (MIR): Similar to QPA in [29], and DA-solution in [30], this method adopts a greedy algorithm to maximize the RIE increment of maintained SILs without considering the task cost. Thus, it selects the task with the maximum value of the RIE one by one until reaching the travelling distance's constraint of each participant.

2) Minimize the Total Cost (MTC): This method also adopts a greedy algorithm to minimize the travelling distance of each participant without considering the RIE increment. Thus, it greedily selects the tasks with the shortest distance within the constraint of each participant's travelling distance.

3) Location-based Task Allocation (LTA): Similar to DBA [29], this method directly calculate the distance between participant and task with Euclidean distance. Then, the computed distance is put into the utility function to allocate tasks. Finally, according to the results of task allocation, the POPP is used to calculate the actual distance for further comparison.

TABLE IV
PARAMETER SETTINGS FOR GENERATING SIMULATION DATA

Parameters	Values	unit
Speed	[0.8, 1.5]	*m/s*
Pause time	[0.8, 1.5]	*s*
Walk time	[2, 6]	*s*
Direction	[-180 180]	°
Simulation time	1000	*s*
Number of nodes	20	/
Time step	1	*s*

B. Simulation Data and Experimental Settings

1) Simulation Data: To evaluate our proposed algorithms, we integrate Random Way Point (RWP) [2] [31] mobility model with the established farmland model to generate the data for evaluating the performance of proposed algorithms. As shown in Fig. 5, the stars, the circles, and the rhombus present the deployment location of SILs, the initial location of participants, and the destination of participants, respectively. Besides, the different colours present different participants, which are randomly generated and can only move in the orange colour area (village) and the gray colour area (road). It is worth noting that the X and Y coordinates in Fig. 5, Fig. 6, and Fig. 7 merely present the points' positions, e.g., the positions of SILs, without any units. The parameter settings for generating simulation data are listed in Table IV.

TABLE V
THE VALUE OF M FOR SIL l IN DIFFERENT λ

M_l	1	2	3	4	5	6	7	8	9	10
$\lambda = 0.2$	27	22	5	31	25	8	14	19	34	39
$\lambda = 0.3$	40	33	8	46	38	13	21	29	52	58
$\lambda = 0.4$	54	44	10	61	51	17	28	39	69	77
$\lambda = 0.5$	67	56	13	77	64	21	36	49	86	97
$\lambda = 0.6$	80	67	16	92	76	25	43	58	103	116

2) Experimental Settings: MATLAB R2019a carries out the simulations on a laptop with a 64-bits Windows 10 operating system, 16 GB RAM, and 1.80-GHz-Core i7 CPU. For each parameter setting, 50 synthetic data are generated, and results are averaged upon them. We use the method in [32] deploying 40 SILs with location information in the established farmland model. Eq. (1) and Eq. (2) are used to determine both the

[2]The reason for choosing RWP to generate the data is that the movement mode of this mobility model is similar to that of farmers. In RWP, mobile nodes tend to move to the predefined area. Similarly, farmers always tend to go back after leaving their homes.

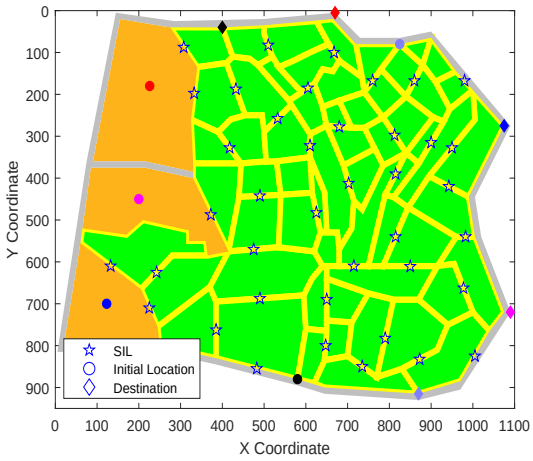

Fig. 5. An illustration of the established farmland model.

number and the location of SILs. Table V (in next page) shows the number M of the pest's carcasses stuck to each SIL in different λ, where the initial number of killed pests is randomly generated between 1 and 200. Table VI (in next page) shows the RIE of each SIL based on the number M_l in different λ. Due to the limited space, we just list the value of both M_l and RIE from s_1 to s_{10}. Here, the value of ϑ is 0.8. Thus, $\lambda \leq 0.8$ denotes that SIL needs to be maintained.

C. Simulation Result

In this part, the ability of CEBT and baseline methods to offer efficient solutions for the SILMP is measured. Furthermore, the influence of task completion rate (TC), the ratio of increased RIE of completed tasks to total RIE increment (RIT), the average distance to perform each task (AD), and average utility value of all completed tasks (AU) is tested as well. The average experimental results of 50 independent simulations are listed in Table VII, where the value of λ varying from 0.2 to 0.6. As mentioned above, λ represents the adherence rate of killed pests. Its value is vulnerable to environmental effects, e.g., humidity and temperature, and varies even in different seasons and same region. Hence, we set the different values of λ to evaluate the effectiveness of the proposed algorithms.

1) Path Planning with Different Participants and RoI: As mentioned before, one of the important properties of our optimisation method is to plan the path for participants from an initial location to the RoI in farmland. In this part, Fig. 6 and Fig. 7 plot the implementation of planned path for these four task allocation algorithms[3], MIR, MTC, LTA, and CEBT with $\lambda = 0.4$, $N_p = 5$, $N_t = 20$, $D = 2.5 \times 10^3$ m, where N_t represents the number of published tasks and D represents the travel distance budget of each participant. Considering the mobility of participants and the irregular distribution of pests, although the parameter settings are same for these two figures, we set different initial location for participants and RoI. In Fig. 6, matching the participants with the RoI of corresponding color clearly shows the allocation results and path planning for each participant. Compared Fig. 6 with Fig. 7, it can be summarized that the task completion rate in Fig. 7 for each method is better than that in Fig. 6, which prove the different participants and RoI in same parameter settings do affect the final results. Although the performance of CEBT in Fig. 6 is worse than that in Fig. 7, it is still superior to other baseline methods in the same experiment.

2) Task Completion Rate: Fig. 8 plots the simulation results of average CR for four methods with $\vartheta = 0.8$, $D = 2.5 \times 10^3$ m, λ increasing from 0.2 to 0.6. The value of CR is a crucial indicator that can reflect the completion status of maintenance tasks visually. In Fig. 8, it can be observed that the CR for all these four methods decreases with the λ increase. However, it is obvious that CEBT and MTC significantly outperform MIR and LTA.

3) The Ratio of Increased RIE of Completed Tasks to Total RIE Increment: Fig. 9 plots the simulation results of average RIT for four methods with the same parameter settings as Fig. 8. The value of RIT reflects the quality of finished tasks. The larger value of the RIT represents that the SIL has a higher priority to be maintained (corresponding task quality is higher). That is no doubt that our CEBT significantly outperform others. Although the MIR is to maximum RIE, its RIT value is still the worst since this method plans many duplicate paths for a participant when he/she is executing the allocated tasks. Furthermore, this issue is more evident with the increase of the total quantity of the tasks, which can be proved based on the results of Fig. 8 and Fig. 10.

4) Travelling Distance: Fig. 10 shows the simulation results of AD for four methods. The value of AD determines the total task cost directly. We notice that the MTC has the shortest average distance for performing a task, which means that the cost to perform each task is optimal. This is indeed justified since the optimisation objective is to prioritise the task with the shortest distance. Although the CEBT is not best, this paper aims to keep the deployed SILs efficiently. Hence, we need to analyse all the experimental results synthetically.

5) Utility Value: Fig. 11 presents simulation results normalisation of AU for four methods with the same parameter settings to Fig. 8. The value of utility represents the trade-off between insecticidal efficiency and total task cost (travelling distance). The utility value is normalised since the dimensional units between RIE and distance are different. Fig. 11 shows that the CEBT is the best solution considering all experiment results synthetically. The most significant difference between the LTA and the CEBT is using two methods to calculate the distance between the task and the participant's current location. Our proposed CEBT significantly outperforms the LTA, indicating the Euclidean distance cannot be used to the actual distance between participants and RoIs directly, especially in an actual farmland scenario.

VI. Conclusion and Future Work

A. Conclusion

Due to the existing problems in SIL-IoT maintenance and the lack of ridges information in commercial maps, we

[3]The simulation data of Fig. 6 and Fig. 7 can be found in the following URL: http://nljrc.njau.edu.cn/index.php/mcs-simulation-dataset/.

TABLE VI
THE RIE IN DIFFERENT λ

RIE_l	1	2	3	4	5	6	7	8	9	10
$\lambda = 0.2$	86.50	89.00	97.50	84.50	87.50	96.00	93.00	90.50	83.00	80.50
$\lambda = 0.3$	80.00	83.50	96.00	77.00	81.00	93.50	89.50	85.50	74.00	71.00
$\lambda = 0.4$	73.00	78.00	95.00	69.50	74.50	91.50	86.00	80.50	65.50	61.50
$\lambda = 0.5$	66.50	72.00	93.50	61.50	68.00	89.50	82.00	75.50	57.00	51.50
$\lambda = 0.6$	60.00	66.50	92.00	54.00	62.00	87.50	78.50	71.00	48.50	42.00

TABLE VII
THE AVERAGE EXPERIMENTAL RESULTS

λ, N_t	Methods	$N_p = 5$				$N_p = 10$				$N_p = 15$			
		$CR(\%)$	$RIT(\%)$	$AD(m)$	$AU(\%)$	$CR(\%)$	$RIT(\%)$	$AD(m)$	$AU(\%)$	$CR(\%)$	$RIT^(\%)$	$AD(m)$	$AU(\%)$
$\lambda = 0.2$ $N_t = 8$	MIR	76.25	80.41	1299.59	28.05	98.25	98.61	1239.89	28.06	100.00	100.00	1197.48	26.95
	MTC	92.75	91.85	834.16	30.98	99.75	99.64	868.06	30.08	100.00	100.00	884.31	27.53
	LTA	86.00	87.87	1035.70	26.53	99.75	99.80	1061.60	25.25	100.00	100.00	1045.87	25.59
	CEBT	92.25	91.73	850.81	31.90	99.75	99.75	880.72	31.08	100.00	100.00	844.99	28.32
$\lambda = 0.3$ $N_t = 14$	MIR	41.00	49.03	1172.66	26.53	70.57	76.73	1183.80	26.64	96.14	97.10	1144.53	22.16
	MTC	80.00	67.52	575.97	35.48	99.71	88.09	691.42	31.20	100.00	100.00	700.74	27.70
	LTA	68.86	60.32	1023.40	25.91	84.71	85.98	1022.70	24.61	97.71	97.57	1040.19	23.71
	CEBT	80.43	83.07	718.89	36.11	99.71	99.77	804.96	31.19	100.00	100.00	795.69	29.48
$\lambda = 0.4$ $N_t = 20$	MIR	23.50	30.47	1111.88	26.21	49.20	58.76	1074.96	24.35	77.70	84.05	1056.87	21.09
	MTC	64.30	55.31	431.74	36.82	91.10	78.98	581.18	29.89	99.40	91.04	630.50	30.18
	LTA	39.10	43.86	964.46	25.80	68.60	75.07	945.59	23.68	84.50	86.88	954.53	21.26
	CEBT	71.20	75.25	581.57	39.68	95.70	96.50	645.02	31.19	99.70	99.80	681.16	30.60
$\lambda = 0.5$ $N_t = 26$	MIR	18.69	24.47	1059.18	23.35	37.15	52.69	968.29	22.83	61.00	70.69	1010.71	20.56
	MTC	53.88	40.11	307.21	40.94	84.15	67.80	444.50	31.60	98.54	84.64	535.70	30.57
	LTA	25.31	28.65	928.78	22.26	50.23	60.00	876.51	21.51	70.54	76.46	912.55	20.13
	CEBT	64.15	60.71	494.70	42.26	88.31	90.91	611.18	32.15	98.69	98.98	675.03	31.09
$\lambda = 0.6$ $N_t = 32$	MIR	14.44	20.15	1025.50	19.21	27.25	36.53	907.97	18.83	45.56	57.30	927.78	19.06
	MTC	47.08	30.12	298.97	41.76	80.50	62.64	404.53	33.18	96.56	75.85	482.19	30.91
	LTA	22.69	25.69	896.80	20.55	41.50	45.51	795.61	18.86	56.13	61.09	801.30	18.22
	CEBT	54.69	58.96	410.55	43.82	85.19	87.96	520.78	34.53	97.38	97.99	552.90	31.41

leveraged the concept of MCS to solve the SILMP. In this paper, we have formulated the SILMP as an orienteering and combinatorial optimization problem and proven that it is NP-hard. Motivated by the face routing and the natural partition structure of farmland, we have proposed two algorithms, namely POPP and CEBT, based on the idea of the greedy algorithm to solve these two subproblems. In POPP, we used the right-hand rule to search for the shortest path between the tasks and participants under the constraint of travelling distance. In CEBT, we proposed a utility function to find a trade-off between the RIE and the task cost. Simulation results verified that our proposed method achieves better performance than the other three baseline methods, synthetically considering the TC, RIT, AD, and AU.

B. Future Work

In this paper, we only consider farmers to be participatory participants in the maintenance task. Farmers, as landowners, are typically required to visit their farms to observe growing progress of crops. In the future, we will consider a hybrid task allocation method to further reduce maintenance costs and improve maintenance efficiency. In addition, participants receive incentive rewards proportional to their travel distances, but, differentiated rewards should be investigated to solve the problem that some tasks are difficult to complete due to far away from villages.

ACKNOWLEDGMENT

This work was supported in part by the National Natural Science Foundation of China under Grant 62072248, in part by China Scholarship Council (CSC) No. 202006850075, and in part by the Jiangsu Agricultural Science and Technology Innovation Fund under Grant CX(21)3060.

REFERENCES

[1] K. Li, L. Shu, K. Huang, Y. Sun, F. Yang, Y. Zhang, Z. Huo, Y. Wang, X. Wang, Q. Lu, and Y. Zhang, "Research and prospect of solar insecticidal lamps internet of things", *Smart Agriculture*, Vol. 1, No. 3, pp. 13-28, 2019. (In Chinese with English abstract).

[2] Y. Liu, X. Ma, L. Shu, G. Hancke, and A. M. Abu-Mahfouz, "From Industry 4.0 to Agriculture 4.0: Current status, enabling technologies, and research challenges", *IEEE Transactions on Industrial Informatics*, Vol. 17, No. 6, pp. 4322-4334, 2020.

[3] H. Ma, D. Zhao, and P. Yuan, "Opportunities in Mobile Crowd Sensing", *IEEE Communications Magazine*, Vol. 52, No. 8, pp. 29-35, 2014.

[4] R. Ganti, F. Ye, and H. Lei, "Mobile Crowd Sensing: Current state and future challenges", *IEEE Communications Magazine*, Vol. 49, No. 11, pp. 32-39, 2011.

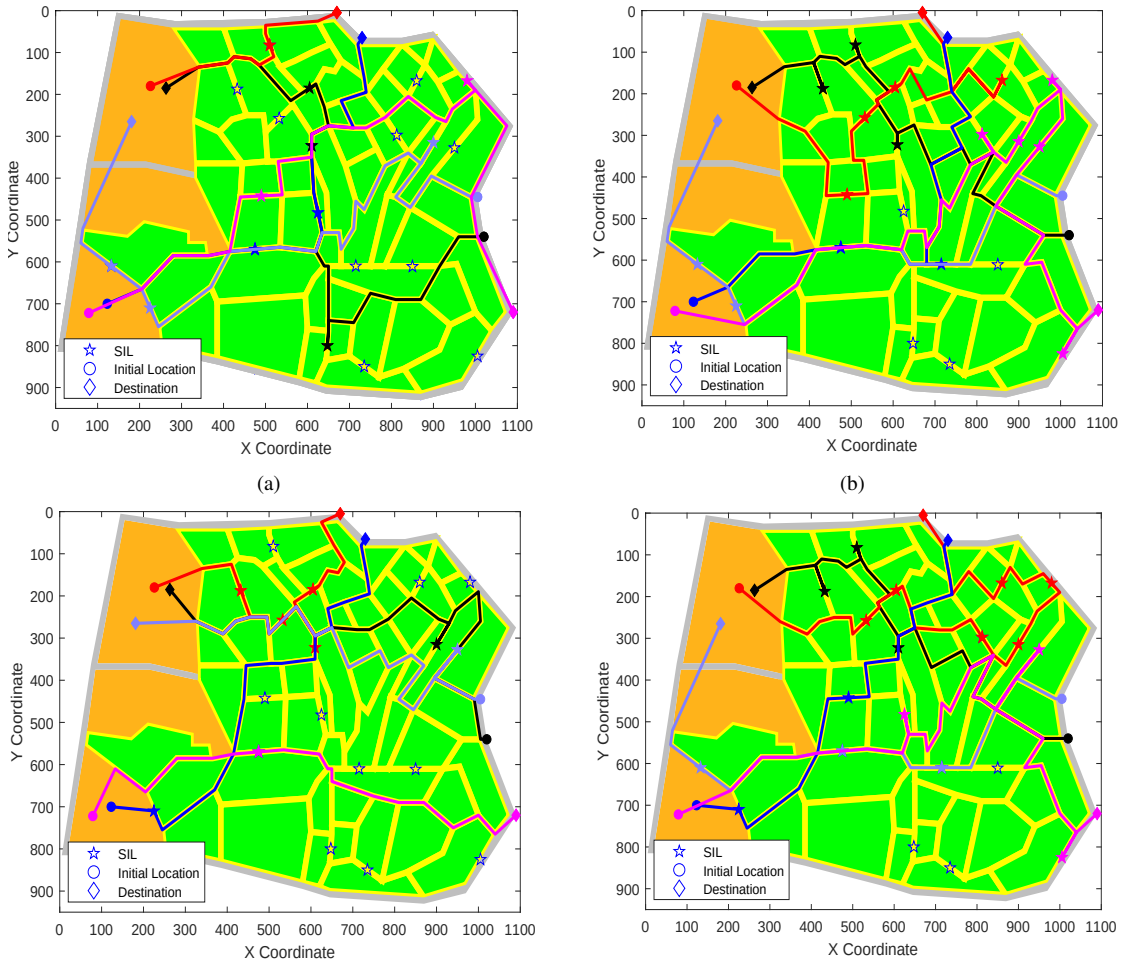

Fig. 6. Allocation results with $\vartheta = 0.8$, $\lambda = 0.4$, $N_t = 20$, $D = 2.5 \times 10^3$ m for experimental synthetic data 1. Synthetic data 1 includes a set of location information, i. e., both the initial location and destination of participants and the location of published tasks. The planned paths and tasks are matched with corresponding participants in the same colour. (a) Allocation results by applying MIR. (b) Allocation results by applying MTC. (c) Allocation results by applying LTA. (d) Allocation results by applying CEBT.

[5] Y. Chen, G. Lee, L. Shu, and N. Crespi, "Industrial internet of things-based collaborative sensing intelligence: framework and research challenges", *Sensors*, Vol.16, No. 2, 2016.

[6] Y. Sun, W. Ding, L. Shu, K. Li, Y. Zhang, Z. Zhou, and G. Han, "On Enabling Mobile Crowd Sensing for Data Collection in Smart Agriculture: A Vision", *IEEE Systems Journal* , 2021. (Early Access)

[7] X. Zhang, Z. Yang, Y. Gong, Y. Liu, and S. Tang, "Spatialrecruiter: Maximizing sensing coverage in selecting workers for spatial crowdsourcing", *IEEE Transactions on Vehicular Technology*, Vol. 66, No. 6, pp. 5229-5240, 2017.

[8] S. He, D. Shin, J. Zhang, and J. Chen, "Toward optimal allocation of location dependent tasks in crowdsensing", *Proc. IEEE INFOCOM 2014-IEEE Conference on Computer Communications*, pp. 745-753.

[9] Y. Liu, B. Guo, Y. Wang, W. Wu, Z. Yu, and D. Zhang, "Taskme: Multi-task allocation in mobile crowd sensing", *Proc. 2016 ACM International Joint Conference on Pervasive and Ubiquitous Computing*, pp. 403-414.

[10] F. Yang, J. Lu, Y. Zhu, J. Peng, W. Shu, and M. Wu, "Heterogeneous task allocation in participatory sensing", *Proc. 2015 IEEE Global Communications Conference*, pp. 1-6.

[11] Y. Kang, X. Miao, K. Liu, L. Chen, and Y. Liu, "Quality-aware online task assignment in mobile crowdsourcing", *Proc. 2015 IEEE 12th International Conference on Mobile Ad Hoc and Sensor Systems*, pp. 127-135.

[12] J. Thebault-Spieker, L. Terveen, and B. Hecht, "Avoiding the south side and the suburbs: The geography of mobile crowdsourcing markets", *Proc. 2015 18th ACM Conference on Computer Supported Cooperative Work & Social Computing*, pp. 265-275.

[13] M. Musthag and D. Ganesan, "Labor dynamics in a mobile micro-task market", *Proc. 2013 SIGCHI conference on human factors in computing systems*, pp. 641-650.

[14] H. Xiong, D. Zhang, G. Chen, L. Wang, and V. Gauthier, "CrowdTasker: maximizing coverage quality in piggyback crowdsensing under budget constraint", *Proc. 2015 IEEE International Conference on Pervasive Computing and Communications*, pp. 55-62.

[15] D. Zhang, H. Xiong, L. Wang, and G. Chen, "CrowdRecruiter: selecting participants for piggyback crowdsensing under probabilistic coverage constraint", *Proc. 2014 ACM International Joint Conference on Pervasive and Ubiquitous Computing*, pp. 703-714.

[16] K. Leyla and C. Shahabi, "GeoCrowd: enabling query answering with spatial crowdsourcing", *Proc. 2012 20th International Conference on Advances in Geographic Information Systems*, pp. 189-198.

[17] T. Hien, L. Fan, L. Tran, and C. Shahabi, "Real-time task assignment in hyperlocal spatial crowdsourcing under budget constraints", *Proc. 2016 IEEE International Conference on Pervasive Computing and Communications*, pp. 1-8.

[18] A. Aleksandar, M. Marjanovic, K. Pripuzic, and I. Zarko, "A mobile crowd sensing ecosystem enabled by CUPUS: Cloud-based publish/subscribe middleware for the Internet of Things", *Future Generation Computer Systems*, Vol. 56, pp. 607-622, 2016.

[19] S. Scellato, A. Noulas, and C. Mascolo, "Exploiting place features in link prediction on location-based social networks", *Proc. 2011 17th ACM SIGKDD international conference on Knowledge discovery and data mining*, pp. 1046-1054.

[20] D. Zhang, H. Xiong, L. Wang, and G. Chen, "CrowdRecruiter: Selecting

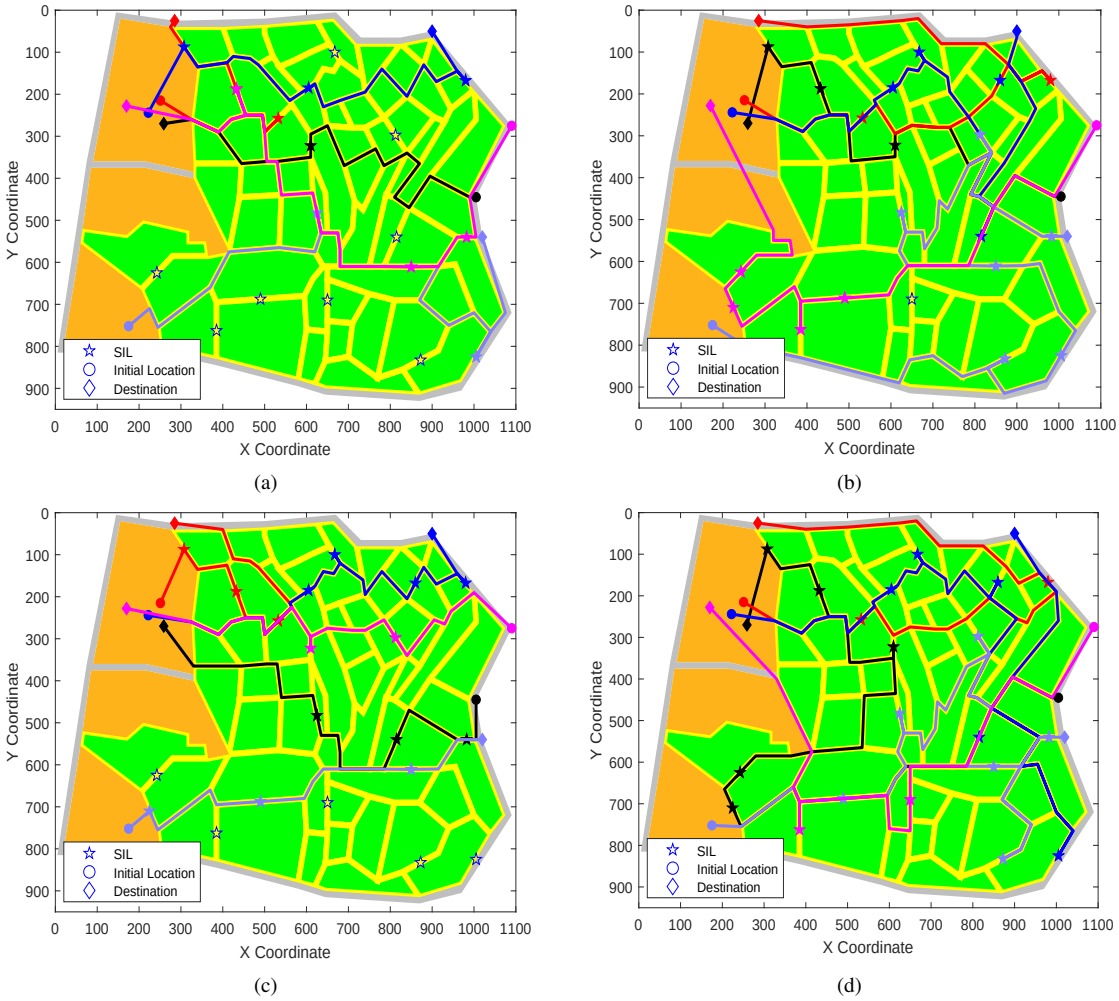

Fig. 7. Allocation results with $\vartheta = 0.8$, $\lambda = 0.4$, $N_t = 20$, $D = 2.5 \times 10^3$ m for experimental synthetic data 2. Synthetic data 2 includes another set of location information, i. e., both the initial location and destination of participants and the location of published tasks. The planned paths and tasks are matched with corresponding participants in the same colour. (a) Allocation results by applying MIR. (b) Allocation results by applying MTC. (c) Allocation results by applying LTA. (d) Allocation results by applying CEBT.

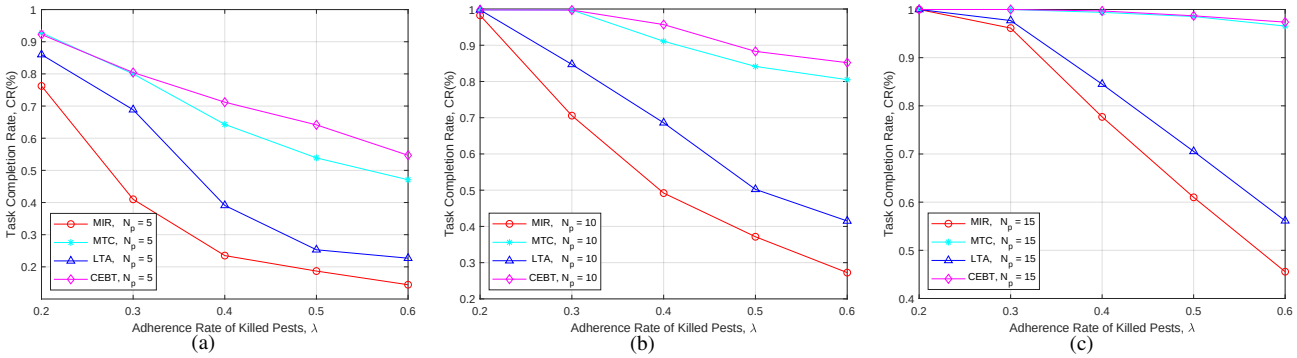

Fig. 8. Average task completion rate (CR) for four methods with $\vartheta = 0.8$, $D = 2.5 \times 10^3$ m, λ from 0.2 to 0.6. (a) Average CR by MIR MTC, LTA, and CEBT with $N_p = 5$. (b) Average CR by MIR MTC, LTA, and CEBT with $N_p = 10$. (c) Average CR by MIR MTC, LTA, and CEBT with $N_p = 15$.

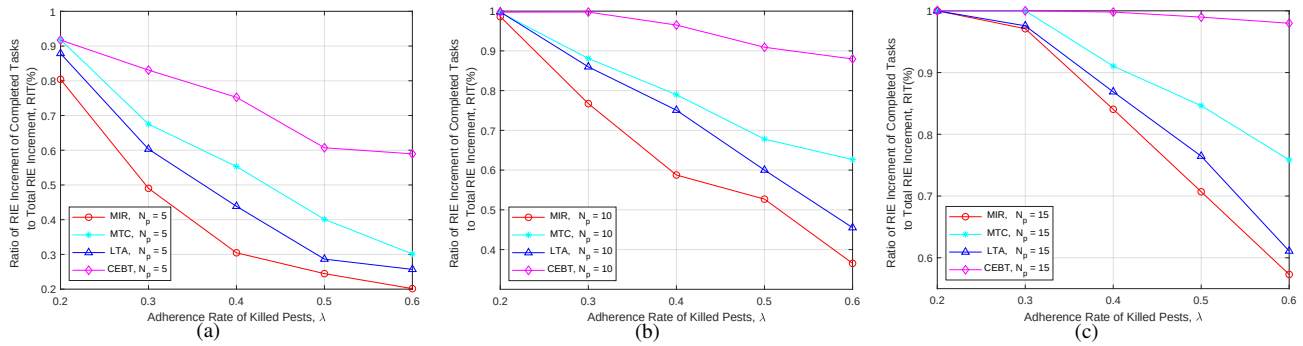

Fig. 9. Average the ratio of increased RIE of completed tasks to total RIE increment (RIT) for four methods with $\vartheta = 0.8$, $D = 2.5 \times 10^3$ m, λ from 0.2 to 0.6. (a) Average RIT by MIR MTC, LTA, and CEBT with $N_p = 5$. (b) Average RIT by MIR MTC, LTA, and CEBT with $N_p = 10$. (c) Average RIT by MIR MTC, LTA, and CEBT with $N_p = 15$.

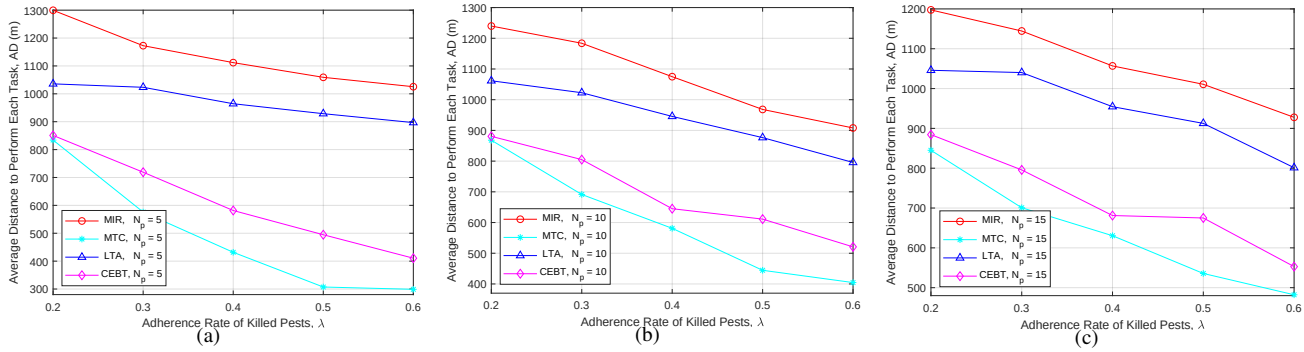

Fig. 10. Average travelling distance per task (AD) for four methods with $\vartheta = 0.8$, $D = 2.5 \times 10^3$ m, λ from 0.2 to 0.6. (a) Average AD by RIT by MIR MTC, LTA, and CEBT with $N_p = 5$. (b) Average AD by RIT by MIR MTC, LTA, and CEBT with $N_p = 10$. (c) Average AD by RIT by MIR MTC, LTA, and CEBT with $N_p = 15$.

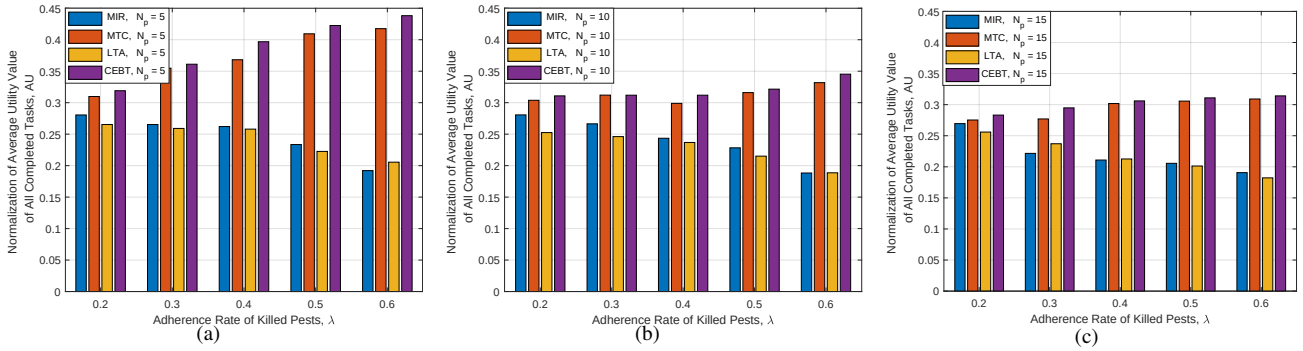

Fig. 11. Normalization of average utility value (AU) for four methods with $\vartheta = 0.8$, $D = 2.5 \times 10^3$ m, λ from 0.2 to 0.6. (a) Normalization of AU by RIT by MIR MTC, LTA, and CEBT with $N_p = 5$. (b) Normalization of AU by RIT by MIR MTC, LTA, and CEBT with $N_p = 10$. (c) Normalization of AU by RIT by MIR MTC, LTA, and CEBT with $N_p = 15$.

participants for piggyback crowdsensing under probabilistic coverage constraint", *Proc. 2014 ACM International Joint Conference on Pervasive and Ubiquitous Computing*, pp. 703-714.

[21] H. Xiong, D. Zhang, G. Chen, L. Wang, V. Gauthier and L. Barnes, "iCrowd: Near-optimal task allocation for piggyback crowdsensing", *IEEE Transactions on Mobile Computing*, Vol. 15, No. 8, pp. 2010-2022, 2016.

[22] J. Wang, Y, Wang, D. Zhang, L. Wang, H. Xiong, A. Helal, H. Duo, F. Wang, "Fine-grained multitask allocation for participatory sensing with a shared budget", *IEEE Internet of Things Journal*, Vol. 3, No. 3, pp. 1395-1405, 2016.

[23] J. Wang, Y, Wang, D. Zhang, F. Wang, Y. He and L. Ma, "PSAllocator: Multi-task allocation for participatory sensing with sensing capability constraints", *Proc. 2017 ACM Conference on Computer Supported Cooperative Work and Social Computing*, pp. 1139-1151.

[24] H. To, M. Asghari, D. Deng, and C. Shahabi, "SCAWG: A toolbox for generating synthetic workload for spatial crowdsourcing", *Proc. 2016 IEEE International Conference on Pervasive Computing and Communication Workshops (PerCom Workshops)*, pp. 1-6.

[25] "GSM/3G/4G-enabled insecticidal lamp", Zhejiang Top Yunnong Technology Co., Ltd, http://www.tpwlw.com/product/cp_84.html, accessed: 2021-06-20.

[26] B. Golden, L. Levy, and R. Vohra, "The orienteering problem", *Naval Research Logistics*, Vol. 34, No. 3, pp. 307-318, 1987.

[27] H. Cho, S. Kim, S. Oh, E. Lee, and S. Kim, "Energy-Efficient and Reliable Face-Routing Scheme in Wireless Networks", *Sensors*, Vol. 21, No. 8, pp. 2746, 2021.

[28] Y. Zhao, J. Zhang, C. Fu, M. Xu, D. Moritz, and Y. Wang, "KD-Box: Line-segment-based KD-tree for Interactive Exploration of Large-scale Time-Series Data", *IEEE Transactions on Visualization and Computer*

Graphics, 2021.
[29] W. Gong, B. Zhang, and C. Li, "Location-based online task assignment and path planning for mobile crowdsensing", *IEEE Transactions on Vehicular Technology*, Vol. 68, No. 2, pp. 1772-1783, 2018.
[30] T. Xi and W. Song, "Location-dependent task allocation for mobile crowdsensing with clustering effect", *IEEE Internet of Things Journal*, Vol. 6, No. 1, pp. 1029-1045, 2018.
[31] T. Hara, "Quantifying impact of mobility on data availability in mobile ad hoc networks", *IEEE Transactions on Mobile Computing*, Vol. 9, No. 2, pp. 241-258, 2009.
[32] F. Yang, L. Shu, Y. Yang, G. Han, S. Pearson, and K. Li, "Optimal Deployment of Solar Insecticidal Lamps over Constrained Locations in Mixed-Crop Farmlands", *IEEE Internet of Things Journal*, 2021.

BIOGRAPHIES

Yuanhao Sun (yhsun.nau@outlook.com) received the B.S. degree in automation from Nanjing Agricultural University, Nanjing, China, in 2016, and the M.S. degree in agricultural engineering from Nanjing Agricultural University, Nanjing, China, in 2018, respectively. He is currently working towards the Ph.D. degree with the College of Engineering, Nanjing Agricultural University, China and a visiting researcher at the school of Engineering, University of Lincoln, U.K. His research interests include mobile crowd sensing and optimization algorithm.

Edmond Nurellari (enurellari@lincoln.ac.uk) was awarded the Carter Prize for the best Ph. D. thesis, titled "Distributed Detection and Estimation in Wireless Sensor Networks: Resource Allocations, Fusion Rules, and Network Security", in University of Leeds, UK. Since April 2017, Dr. Nurellari has been a faculty member with the School of Engineering at the University of Lincoln, United Kingdom, where he is currently an Associate Professor/Programme Leader in Electrical Engineering/Robotics. His research interests include machine learning, robotics for communications, distributed signal processing, signal processing on graphs, resource allocations and distributed decisions in WSNs. He has served as an Invited Reviewer for the IEEE Trans. on Signal and Info. Process. over Networks, IEEE Communication Letter, Springers Wireless Networks Journal, Springers Digital Signal Processing Journal and IEEE Flagship conferences. Over the past few years, Dr. Nurellari has served as a Guest Editor of Special Issue "Smart Agricultural Applications with Internet of Things" for Sensors Journal, Associate Editor of Special Issue "Towards Next Generation UAV-Enabled Applications: Communication, Sensing and Security", Aerial and Space Networks journal, Editorial Board for Frontiers in Communications and Networks Journal, Journal Topics Board for Journal of Sensor and Actuator Networks, TPC Member for IEEE iSES, International Conference on Smart and Sustainable Agriculture (SSA'2021), and a Reviewer for several UKRI grants including EPSRC and Future Leaders Fellowship.

Weimin Ding (wmding@njau.edu.cn) received the B.S. degree from Anhui Agricultural University, Hefei, China in 1981, the M.S. degree from Nanjing Agricultural University, Nanjing, China in 1984, and the Ph.D. degrees from Nanjing Agricultural University, Nanjing, China in 1999. He is the director of Key Laboratory of Intelligent Agricultural Equipment of Jiangsu Province and is currently a Professor at Nanjing Agricultural University, Nanjing, China. His research interests include smart agriculture and facility agriculture.

Lei Shu (lei.shu@njau.edu.cn) received the B.S. degree in computer science from South Central University for Nationalities, China, in 2002, and the M.S. degree in computer engineering from Kyung Hee University, South Korea, in 2005, and the Ph.D. degree from the Digital Enterprise Research Institute, National University of Ireland, Galway, Ireland, in 2010. Until 2012, he was a Specially Assigned Researcher with the Department of Multimedia Engineering, Graduate School of Information Science and Technology, Osaka University, Japan. He is currently a Distinguished Professor with the Nanjing Agricultural University, China, and a Lincoln Professor with the University of Lincoln, U.K. He is also the Director of the NAU-Lincoln Joint Research Center of Intelligent Engineering. He has published over 400 papers in related conferences, journals, and books in the areas of sensor networks and Internet of Things. His current H-index is 65 and i10-index is 272 in Google Scholar Citation. His current research interests include wireless sensor networks and Internet of Things. He has also served as a TPC member for more than 150 conferences, DCOSS, MASS, ICC, GLOBECOM, ICCCN, WCNC, and ISCC. He has served over 50 various Co-Chair for international conferences/workshops, such as IWCMC, ICC, ISCC, ICNC, Chinacom, especially the Symposium Co-Chair for IWCMC 2012, ICC 2012, the General Co-Chair for Chinacom 2014, Qshine 2015, Collaboratecom 2017, DependSys 2018, and SCI 2019, the TPC Chair for InisCom 2015, NCCA 2015, WICON 2016, NCCA 2016, Chinacom 2017, InisCom 2017, WMNC 2017, and NCCA 2018. He has also served on the Editorial Boards, including the IEEE Transactions on Industrial Informatics, IEEE Communications Magazine, IEEE Network Magazine, IEEE ACCESS, IEEE/CCA JAS. He is also an Editor in Chief of Journal of Sensor and Actuator Networks, a Specialty Chief Editor of Frontiers in Plant Science-Sustainable and Intelligent Phytoprotection.

Zhiqiang Huo (z.huo@ucl.ac.uk) Zhiqiang Huo received the B.S. and M.S. degrees from the China University of Geosciences (Beijing), Beijing, China, in 2013 and 2016, and the Ph.D. degree from the School of Engineering from the University of Lincoln, U.K., in 2020. He is currently a Research Associate with the Institutional Research Information System (IRIS) at the University College London (UCL), London, UK. His research interests include time-series complexity analysis, reliability analysis, data mining, and artificial intelligence. He received the INISCOM 2017 Best Paper Award. He has served as the Co-Chair of international conferences/workshops, such as the AINIS 2016, CollaborateCom 2017, and CIoT 2021. He regularly reviews for leading journals such as IEEE Transactions on Industrial Informatics, IEEE-CAA Journal of Automatica Sinica, and IEEE Sensors.